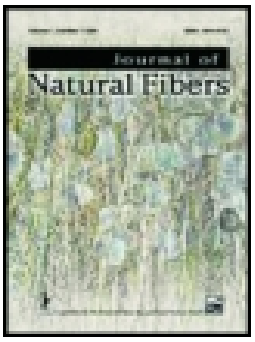

Taylor & Francis
Taylor & Francis Group

Journal of Natural Fibers

ISSN: (Print) (Online) Journal homepage: https://www.tandfonline.com/loi/wjnf20

An investigation of the effects of extraction and brushing variables on the properties of hedge sisal fibers using a raspador

N. W. Barasa, K. D. Njoroge & T. O. Mbuya

JOURNAL OF NATURAL FIBERS
https://doi.org/10.1080/15440478.2020.1870641

ARTICLE

Check for updates

An investigation of the effects of extraction and brushing variables on the properties of hedge sisal fibers using a raspador

N. W. Barasa, K. D. Njoroge, and T. O. Mbuya

Department of Mechanical Engineering, University of Nairobi, Nairobi, Kenya

ABSTRACT

Natural fibers have emerged as an important component in the development of composite materials because of their mechanical properties. The properties are highly influenced by environmental conditions and processing techniques. This variability makes their usability in reinforcement unpredictable. There are satisfactory attempts to quantify the variation of the properties with environmental conditions. However, the quantification of how the properties vary with processing methods is unsatisfactory. This study, therefore, investigated and quantified the effects of processing variables on the properties of sisal fibers using a raspador. The raspador was designed, fabricated, and utilized in processing sisal fibers. Processing variables such as gap size, number of extraction and brushing elements, and drum speed were investigated. The mechanical properties were determined based on ASTM C1557 standard. High correlation coefficients were found between fiber properties and the processing variables. The brushing process, mostly ignored in many cases, improved the properties of the sisal fibers.

摘要

天然纤维因其优异的力学性能而成为复合材料发展的重要组成部分. 其性能受环境条件和加工工艺的影响很大. 这种可变性使得它们在加固中的可用性无法预测. 有令人满意的尝试, 以量化的变化与环境条件的性质. 然而, 量化的性质如何随加工方法的变化是不令人满意的. 因此, 本研究以剑麻纤维为研究对象, 利用拉斯帕刀, 探讨并量化了不同加工参数对剑麻纤维特性的影响. 设计、制造并应用于剑麻纤维加工. 研究了间隙大小、萃取和刷洗元件的数量以及滚筒转速等工艺参数. 力学性能按ASTM C1557标准测定. 纤维性能与加工变量之间有很高的相关系数. 在许多情况下, 刷毛工艺往往被忽略, 从而改善了剑麻纤维的性能.

KEYWORDS
Brushing; extraction; fiber properties; raspador; sisal; variation

关键词
疾驰的; 提取; 纤维性能; 拉斯帕多; 剑麻; 变异

Introduction

Sisal fibers are among the natural fibers that have the highest mechanical properties (Mutuli, Bessell, and Talitwala 1982). The fiber is obtained from sisal, a succulent hardy cactus plant composed of sword-shaped leaves. The plant copes substantially with a wide range of warm climatic conditions experienced in arid and semi-arid lands (ASALs[1]) (Kayumba et al. 2007). Among the leading commercial varieties are Agave sisalana and Agave fourcroydes.

Sisal fibers are composed of a bundle of multicellular hollow sub-fibers held together by a matrix composed of hemicellulose and lignin (Petroudy 2017). The cellulose microfibrils play a key role in reinforcing natural fibers. The fiber fails if the matrix is debonded from the reinforcing fibrils. Microfibrillar angle,[2] cell dimensions, defects, and chemical composition are important determinants of fiber properties (Petroudy 2017; Zhu, Hao, and Zhang 2018). The amount of cellulose and degree of crystallinity highly influence the mechanical properties of the fibers. These antecedents are further

CONTACT N. W. Barasa nelsonlyton@gmail.com Department of Mechanical Engineering, University of Nairobi, Nairobi, Kenya.

influenced by chemical and physical surface modifications, environment conditions, and processing methods (Fidelis et al. 2013; Kithiia, Munyasi, and Mutuli 2020; Mohammed and Chan 2008; Petroudy 2017; Silva, Chawla, and Filho 2008).

Sisal fibers have attracted attention from scholars in the development of polymer composites (Kithiia, Munyasi, and Mutuli 2020; Majesh and Pitchaimani 2016; Rajkumar, Santhy, and Padmanaban 2020; Susheel, Kaith, and Inderjeet 2009). This is due to their good mechanical properties, disposability, availability, affordability, and friendliness to the environment and users (Bhowmicka, Mukhopadhyayb, and Alagirusamyb 2012; Gobikannan et al. 2020; Rajkumar, Santhy, and Padmanaban 2020). However, for effective utilization of the fibers for reinforcement purposes, there is a need to quantify the variability of their mechanical properties (Abir, Kashif, and Razzak 2015).

Most of the research done so far has focused on determining the variation of the fiber properties with surface modifications (Kithiia, Munyasi, and Mutuli 2020; Mokaloba and Batane 2014; Zhu, Hao, and Zhang 2018). The variability due to other physical factors such as gauge length, morphology, and temperature have also been quantified (Abir, Kashif, and Razzak 2015; Fidelis et al. 2013; Jain, Banerjee, and Sanyal 2012; Kithiia, Munyasi, and Mutuli 2020; Silva, Chawla, and Filho 2008). For instance, Jain, Banerjee, and Sanyal (2012) and Silva, Chawla, and Filho (2008) quantified the variation of tensile strength and Young's modulus of coir and sisal fibers with gauge length and found it to be negligible. However, the properties vary with the leaf section with the mid-section having the highest properties followed by the tail end and the butt end in that order (Abir, Kashif, and Razzak 2015; Mohammed and Chan 2008).

There is, however, inadequate research on the quantification of the variability of the fiber properties with extraction and processing methods despite acknowledgment of their influence by scholars like Abir, Kashif, and Razzak (2015); Naik, Dash, and Goel (2013); Silva, Chawla, and Filho (2008). Naik, Dash, and Goel (2013) research quantified the variation of sisal fiber properties with harvesting and processing conditions but did not investigate the effect of processing variables such as gap size, machine speed, and the number of blades or elements.

Since every natural fiber must be processed before utilization, there is still a need to understand the effect of processing variables on fiber properties. The surface modification only improves the fiber properties obtained after processing. Extraction and brushing are two important fiber processing activities whose effect on the fiber properties cannot be ignored. Due to inadequate research in this domain, the objective of this work was to investigate and quantify the variation of the tensile properties of untreated sisal fibers with extraction and brushing variables using raspador.[3]

Materials and methods

Materials

The raspador for extraction and brushing of sisal fibers; is a 3 Hp small machine with a processing capacity of 24 kg dry fiber per hour. It is designed with a variable drum speed (900–1500 rpm), gap size (0–5 mm), and blades/brushing elements (3, 6, and 12 uniformly distributed on 457.2 mm drum's circumference). The extraction and brushing units are 150 mm and 250 mm long, respectively.

Hounsfield Tensometer (Type W) for tensile tests (Figure 2); it has wedge-shaped self-aligning jaws that increase grip in accordance with the applied force. Tensile results are read from an autographic recorder at different magnifications (1–16). It has strain rates of 1.6 mm/min, 3.2 mm/min, and 6.4 mm/min.

LV 800AT Tester for determination of fiber diameters; it is embedded with an optic microscope and micrograph characterization software capable of determining the fiber diameters within a tolerance of 0.01 μm.

Other important materials required were 3-year-old hedge sisal from Nairobi, Kenya; an electric oven with 1°C/min heating rate; emery paper and wood glue for preparation of samples.

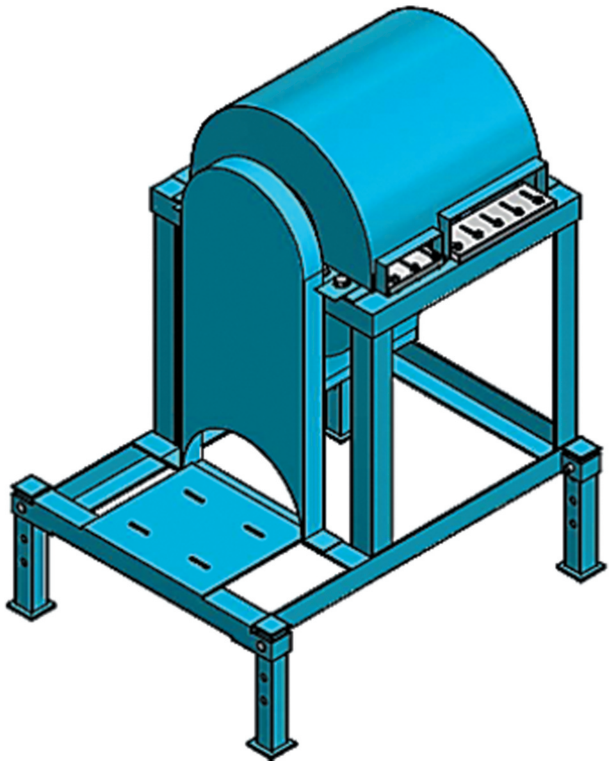

Figure 1. The design of the raspador.

Methods

An experimental research design was employed in this study. A raspador (Figure 1) for extraction and brushing of sisal fibers was designed based on the raspador principle. An important design equation relating speed, the rate of feeding, and the number of blades/brushing elements to extraction/brushing quality (equation 1) was derived from the principle. This equation applies to all other natural fibers as long as their extraction process is designed based on the raspador principle. However, the exact sensitivity of these variables to other natural fibers can be quantified experimentally.

$$\delta = \frac{2\pi c}{n\omega} \tag{1}$$

where:

δ – Pitch (an indicator of processing quality)
c – Rate of feeding
n – Number of extraction blades/brushing elements
ω – Drum speed

An equation relating the power consumption, drum speed, and radius of the raspador was also established (equation 2). Equations 1 and 2 were used to size the important parts of the machine such as drum (457.2 mm outer diameter, 400 mm long and 3 mm thick), motor (3 Hp), and blades (38*38*5 mm). See Appendix A, Figure A1 and A2 for important dimensions of the raspador.

$$P = (D_R)_e \omega R_O \tag{2}$$

where:

P – Power required

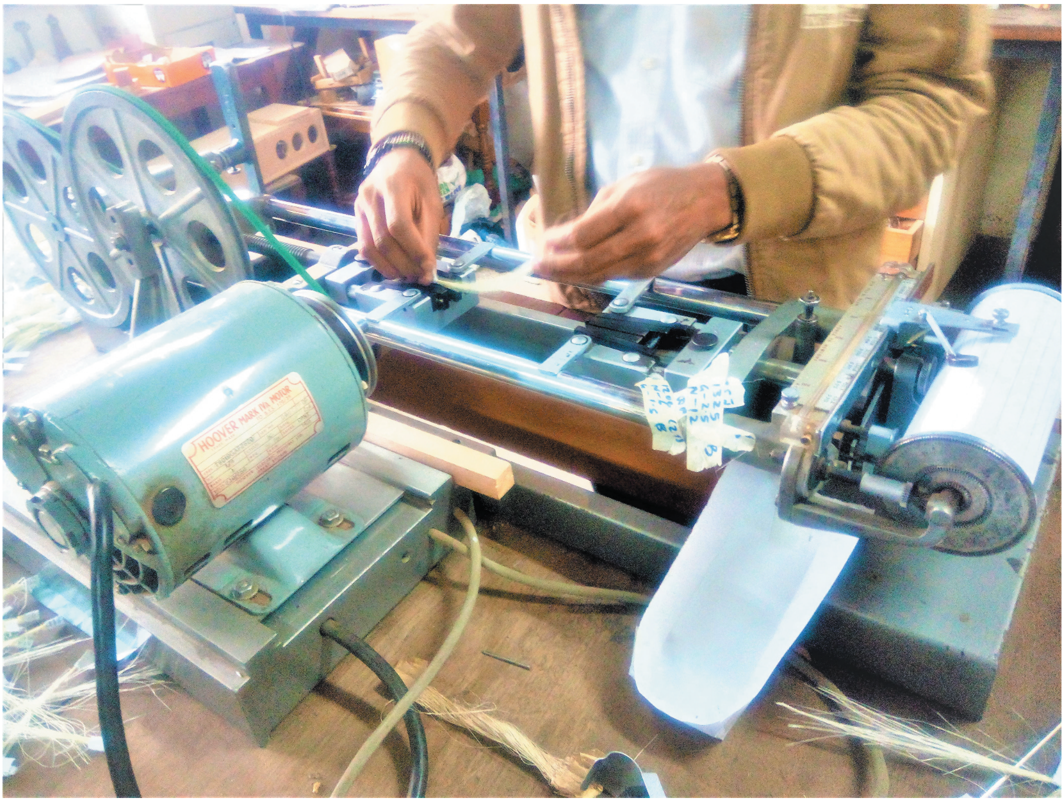

Figure 2. Fiber testing using Hounsfield Tensometer (Type W).

$(D_R)_e$ – Decortication resistance

R_O – Drum radius

The designed raspador (Figure 1) was fabricated at Mechanical Engineering Workshop, University of with allowances to vary ω, n and gap size that are the important parameters under investigation.

To limit variabilities in fiber properties caused by environmental conditions (Abir, Kashif, and Razzak 2015), all the hedge sisal was obtained at Kasarani constituency in Nairobi, Kenya.[4] The sisal leaves were extracted within 24 hours after harvesting to minimize fiber degradation. By holding other factors constant, the leaves were extracted first at different gap size, then the number of blades and machine speed. Thereafter, the fibers were then dried in the sun for 3 days before samples were randomly taken for preparation of extraction process specimens. After the third day, the fibers were also brushed at different gap sizes, number of brushing elements, and machine speed.[5] Similarly, brushing process samples were randomly selected using stratified random sampling to ensure an equal likelihood of sampling a fiber strand from the sisal hunk (Denscombe 2010). This limited the effect of inverse proportionality between strength and diameter of the fibers (Ferreira, Ferreira, and Monteiro 2018) because the properties of natural fibers vary from one plant or strand to the other.

Fibers of length 150 mm were cut from the butt-end section. A total of 40 fiber strands were randomly picked and glued to a gauge length of 140 mm using emery paper and wood glue and allowed to cure for 24 hours. Forty strands were used because preliminary results by Kithiia, Munyasi, and Mutuli (2020) showed that better tensile test results for untreated sisal fibers are achieved at 40 strands. Since results also show that the variation of tensile properties with gauge length within a given portion of the fiber is negligible (Jain, Banerjee, and Sanyal 2012; Silva, Chawla, and Filho 2008), a gauge length of 140 mm was preferred for machine convenience but constrained to the butt-end region to minimize any variations since the properties vary with leaf section (butt end, mid end and tail end). To counter the variability due to moisture content (Abir, Kashif, and Razzak 2015), all samples were dried in an electric oven at a rate of 1°C/min for 30 minutes prior to testing. The fibers were then left to cool to room temperature while in the oven to minimize thermal shocks.

The tensile tests were performed using Hounsfield Tensometer (Type W) (Figure 2) at a room temperature ranging between 22°C and 24°C and average relative humidity of 60%. A constant strain rate of 3.175 mm/min and a magnification of x8 were used. The fracture load and deformation were determined from the load-deformation plots generated. The actual deformation was obtained by dividing the elongation measured on the plot by the magnification factor (x8).

A total of 160 samples were tested to determine the variation of the fiber properties with the processing variables. This sample size ensured that for every datapoint, a total of six specimens were tested. This is a good sample size given that every specimen had 40 strands in total; hence, the result was an average of 40 fibers. If a single fiber strand was used, the sample size would need to be too large to increase the level of confidence in the result. All the results are presented with population standard deviation (SD) determined from equation 3.

$$\sigma = \sqrt{\frac{1}{N}\sum_{i=1}^{N}(x_i - \mu)^2} \tag{3}$$

where:

σ – SD

N – Population

x_i – i^{th} value

μ – Mean

A total of 21 samples were used to determine the mean fiber diameter using the optic microscope embedded in the LV 800AT Tester. The data collected were analyzed using equations 4 to 7. The fracture stress, elastic modulus, and fracture strain were determined as specified in the ASTM C1557 standard (ASTM 2008).

Fiber fracture/ultimate stress

$$\sigma_{\mathrm{u}} = \frac{\mathrm{Breakingload}}{\mathrm{Crosssectionarea}} \tag{4}$$

Fracture strain

$$\varepsilon = \frac{\mathrm{Deformation}}{\mathrm{Gaugelength}} \tag{5}$$

Modulus of elasticity

$$\mathrm{E} = \frac{\sigma_{\mathrm{u}}}{\varepsilon} \tag{6}$$

Cross-section area

$$\mathrm{A} = \frac{\pi \mathrm{d}^2}{4} \tag{7}$$

Results and discussion

Due to the great variations in the morphology of sisal fibers, 21 samples were used to determine the average fiber diameter in μm. The average butt-end diameter of the unbrushed sisal fibers was 279.55 ± 5.66 μm whereas for the brushed fibers was 251.05 ± 4.26 μm. These diameters are within the range of 192.65–396.8 μm reported by Kithiia, Munyasi, and Mutuli (2020) for Kenyan sisal fibers.

Table 1. Effect of gap size on tensile properties of sisal fibers.

Extraction Blades/ Brushing elements	Machine speed (rpm)	Gap Size (mm)	Fracture stress (MPa)		Fracture strain		Young's modulus (GPa)	
			Extraction	Brushing	Extraction	Brushing	Extraction	Brushing
3	1400	1.0	120.6 ± 11	134.9 ± 18	0.097 ± 0.001	0.088 ± 0.005	1.25 ± 0.16	1.53 ± 0.17
		1.5	122.2 ± 1	144.5 ± 15	0.092 ± 0.002	0.084 ± 0.001	1.34 ± 0.23	1.75 ± 0.17
		2.0	123.6 ± 5	147.7 ± 15	0.089 ± 0.004	0.083 ± 0.004	1.38 ± 0.02	1.79 ± 0.12
		2.5	126.2 ± 4	148.2 ± 9	0.079 ± 0.000	0.081 ± 0.001	1.59 ± 0.04	1.83 ± 0.14
		3.0	132.3 ± 17	147.7 ± 17	0.087 ± 0.001	0.078 ± 0.003	1.52 ± 0.22	1.89 ± 0.17
		3.5	135.4 ± 4	166.6 ± 20	0.084 ± 0.001	0.072 ± 0.004	1.63 ± 0.04	2.38 ± 0.20

Key: ± – Standard deviation from 6 samples

Table 2. Effect of extraction blades and brushing elements on tensile properties of sisal fibers.

Machine speed (rpm)	Gap Size (mm)	Extraction Blades/ Brushing elements	Fracture stress (MPa)		Fracture strain		Young's modulus (GPa)	
			Extraction	Brushing	Extraction	Brushing	Extraction	Brushing
1400	2.5	3	126.2 ± 4	148.2 ± 9	0.0790 ± 0.000	0.081 ± 0.001	1.59 ± 0.04	1.83 ± 0.14
		6	120.1 ± 4	146.3 ± 1	0.0795 ± 0.001	0.084 ± 0.003	1.51 ± 0.05	1.78 ± 0.05
		12	99.6 ± 11	144.2 ± 4	0.0800 ± 0.016	0.096 ± 0.002	1.24 ± 0.26	1.50 ± 0.02

Key: ± – Standard deviation from 6 samples

Table 3. Effect of machine speed on tensile properties of sisal fibers.

Extraction Blades/ Brushing elements	Gap Size (mm)	Machine speed (rpm)	Fracture stress (MPa)		Fracture strain		Young's modulus (GPa)	
			Extraction	Brushing	Extraction	Brushing	Extraction	Brushing
12	2.5	900	165 ± 8	181.8 ± 0.02	0.073 ± 0.002	0.074 ± 0.002	2.30 ± 0.12	2.46 ± 0.2
		1092	119.3 ± 3	117.8 ± 1	0.074 ± 0.002	0.088 ± 0.003	1.61 ± 0.59	1.34 ± 0.06
		1200	109.9 ± 13	114.8 ± 3	0.076 ± 0.001	0.090 ± 0.007	1.44 ± 0.18	1.28 ± 0.10
		1325	102.2 ± 23	131.9 ± 12	0.077 ± 0.000	0.087 ± 0.000	1.33 ± 0.32	1.52 ± 0.14
		1400	99.6 ± 11	144.2 ± 4	0.080 ± 0.016	0.096 ± 0.002	1.24 ± 0.26	1.50 ± 0.02

Key: ± – Standard deviation from 6 samples

The reduction in average diameter after brushing was attributed to the removal of more materials from the fibers to form brush dust.

The effect of gap size on the properties of sisal fibers was first determined while holding the machine speed and number of blades/brushing elements constant. Table 1 presents the mean results obtained when the gap size was varied from 1 to 3.5 mm using 6 samples at every gap size.

Gap sizes between 1.5 and 2.5 mm gave better results when other quality factors such as color and length of fibers were taken into consideration. Based on this, a gap size of 2.5 mm was adopted to determine the effect of extraction blades/brushing elements (Table 2) and drum speed (Table 3) on sisal properties. The holes and blades/elements need to be uniformly distributed on the drum to avoid out of balance masses that would cause machine vibrations. This means that it is only possible to use either a combination of 2, 4, and 8 or 3, 6, and 12 blades/elements, and not both. The latter combination was preferred because it is a good representative of the low, middle, and high number of blades/elements.

It was observed that the fracture stress, elastic modulus, and fracture strain vary with the number of extraction blades/brushing elements, machine speed, and gap size as presented in Table 1–3. The unbrushed fibers had an average fiber length of 1031.3 mm and a length reduction ratio (LR[6]) of 0.912. Moreover, the average length, fracture stress, fracture strain, and modulus of elasticity of 1031.3 ± 6.7 mm, 124.04 ± 19 MPa, 0.085 ± 0.012, and 1.484 ± 0.28 GPa, respectively. However, because the fiber is unbrushed, irrespective of its strength, color, and fiber length, its grade was UHDS according to LSA's (2016) guidelines.[7]

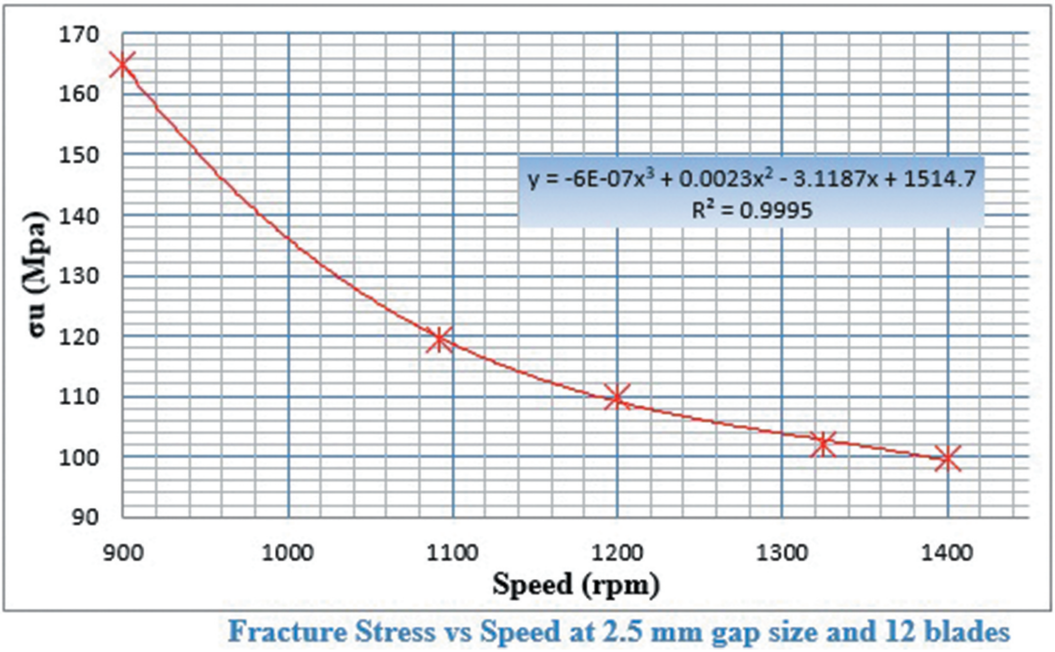

Figure 3. Variation of fracture stress with speed (extraction of fibers at 2.5 mm gap size and 12 blades).

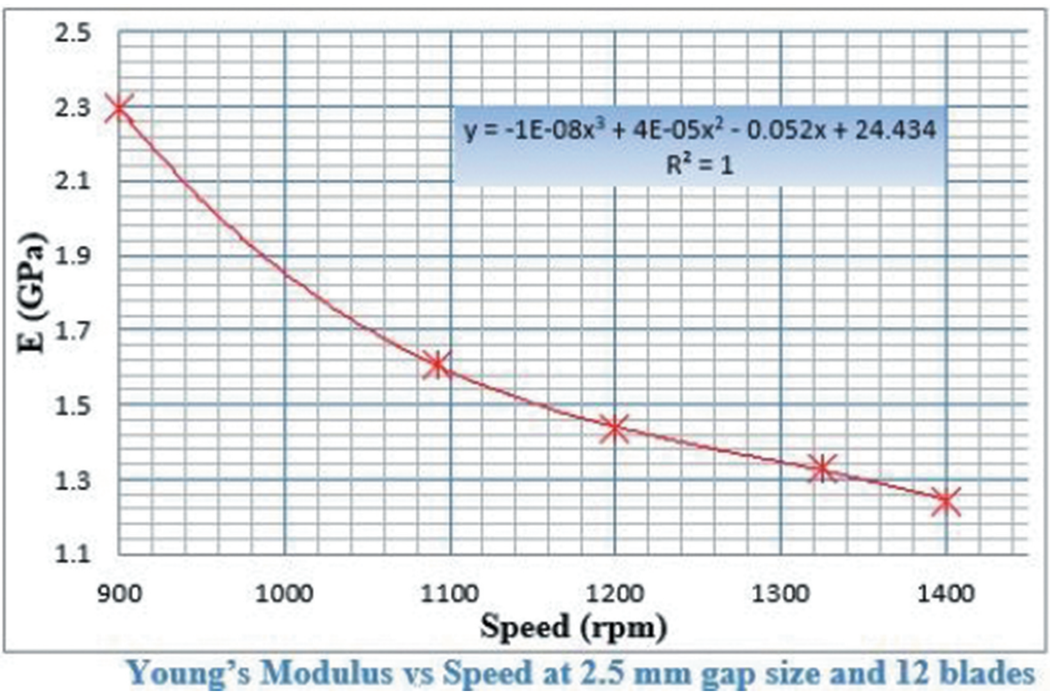

Figure 4. Variation of elastic modulus with speed (extraction of fibers at 2.5 mm gap size and 12 blades).

After brushing, the average fiber length, fracture stress, fracture strain, and modulus of elasticity were 955.2 ± 66.9 mm, 142.68 ± 23 MPa, 0.08118 ± 0.01, and 1.776 ± 0.39 GPa, respectively. These

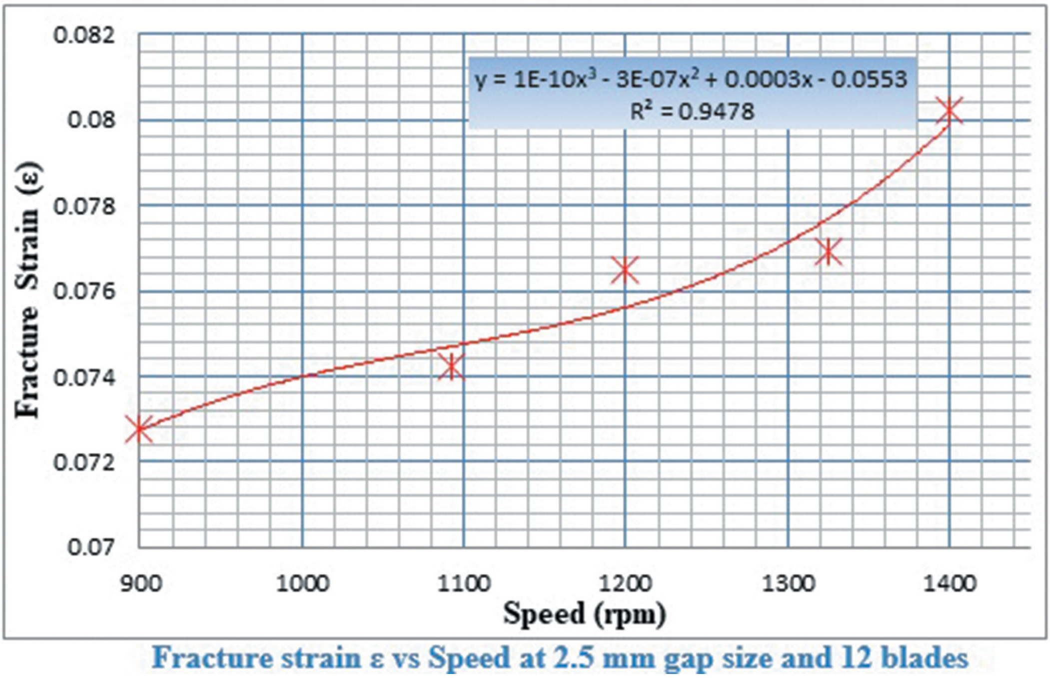

Figure 5. Variation of fracture strain with speed (extraction of fibers at 2.5 mm gap size and 12 blades).

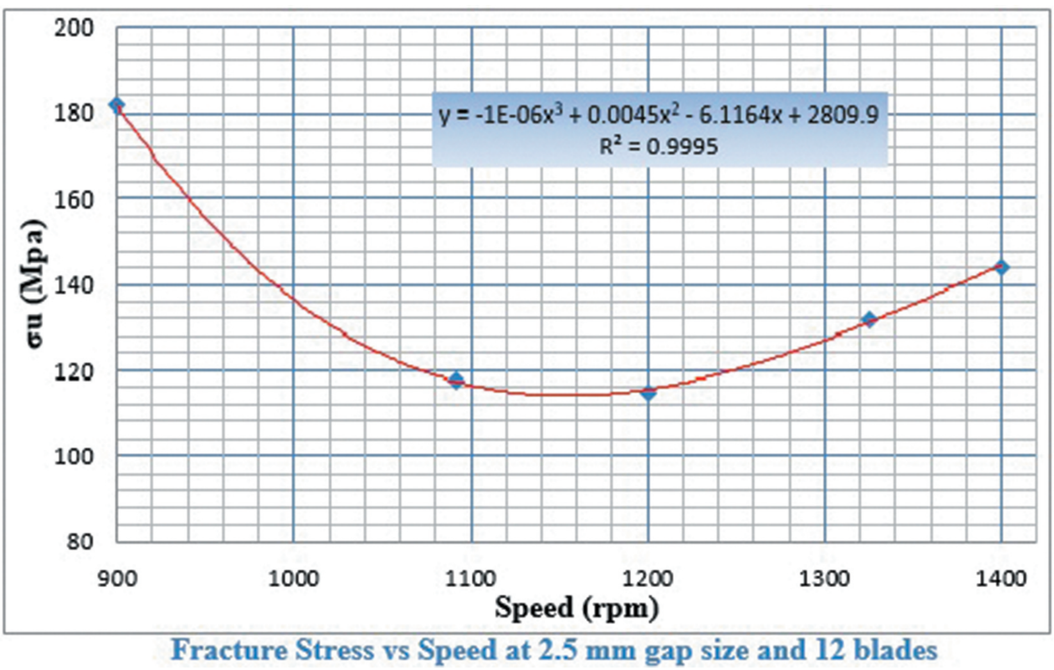

Figure 6. Variation of fracture stress with speed (brushing of fibers at 2.5 mm gap size and 12 brushing elements).

properties are comparable to average butt and mid-section properties of 161 MPa stress, 3.6 GPa modulus, and 4.5% strain obtained by Kithiia, Munyasi, and Mutuli (2020) for Rea Vipingo sisal from Kenya. However, the stress is lower than 410 MPa reported by Phologolo et al. (2012) because they

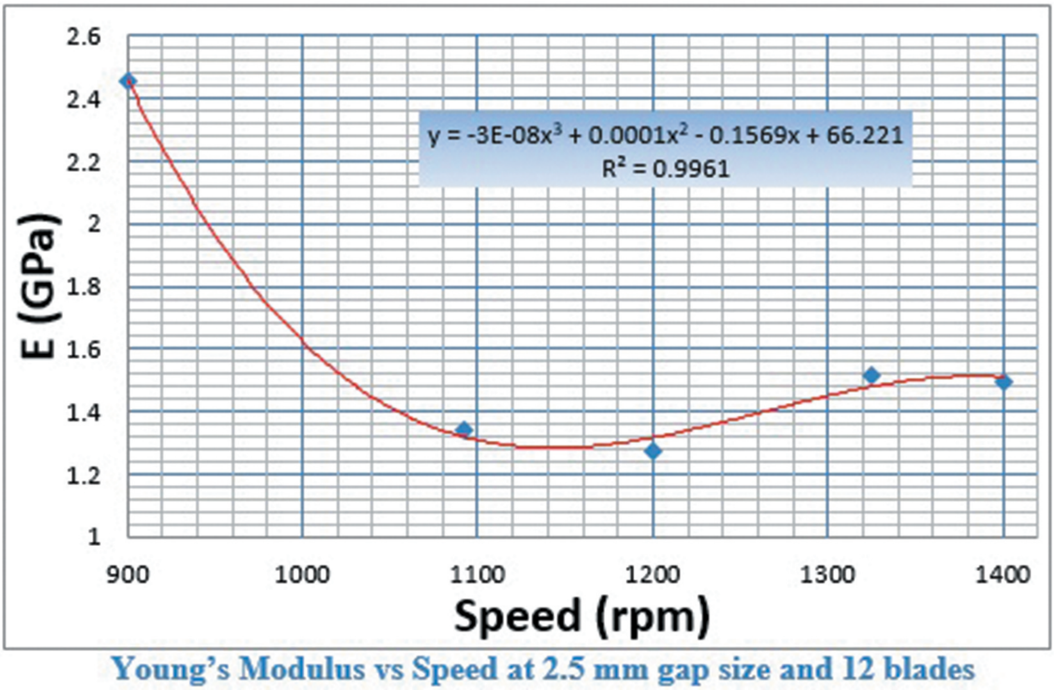

Figure 7. Variation of elastic modulus with speed (brushing of fibers at 2.5 mm gap size and 12 brushing elements).

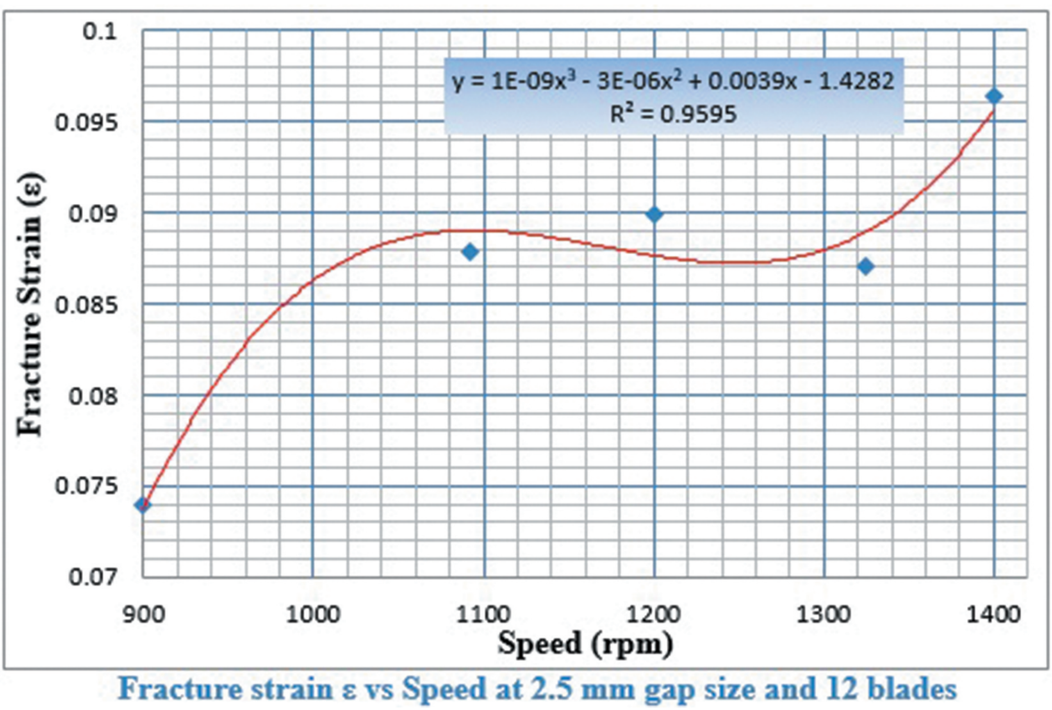

Figure 8. Variation of fracture strain with speed (brushing of fibers at 2.5 mm gap size and 12 brushing elements).

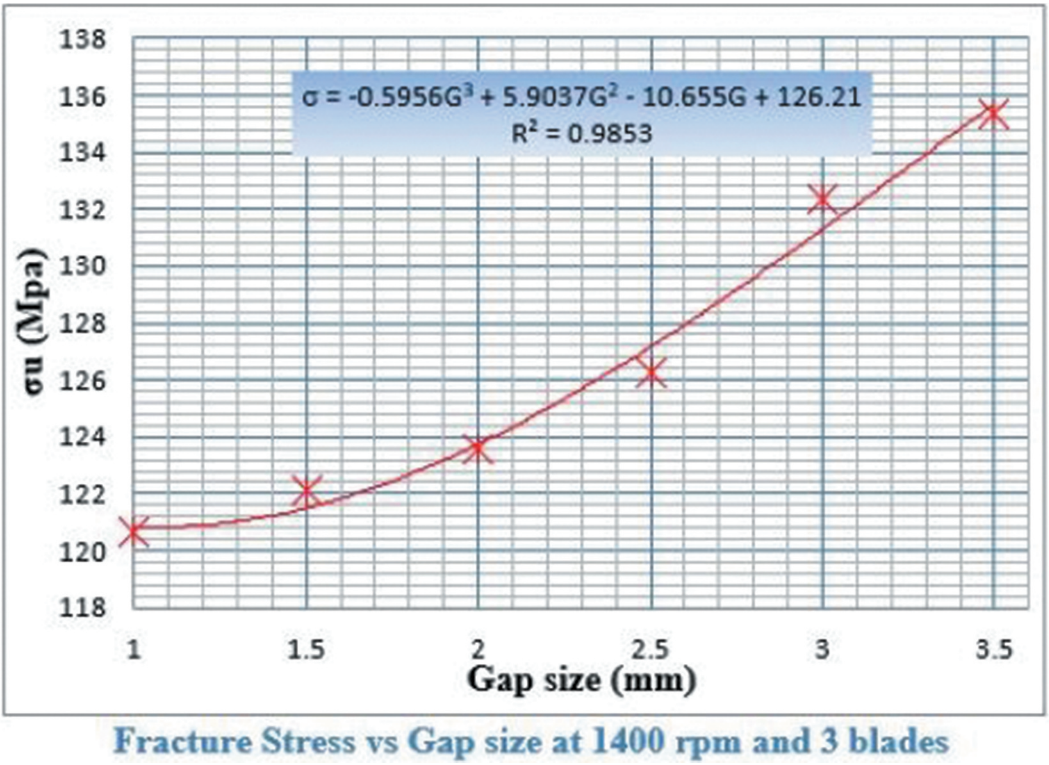

Figure 9. Variation of fracture stress with gap size (extraction of fibers at 1400 rpm and 3 blades).

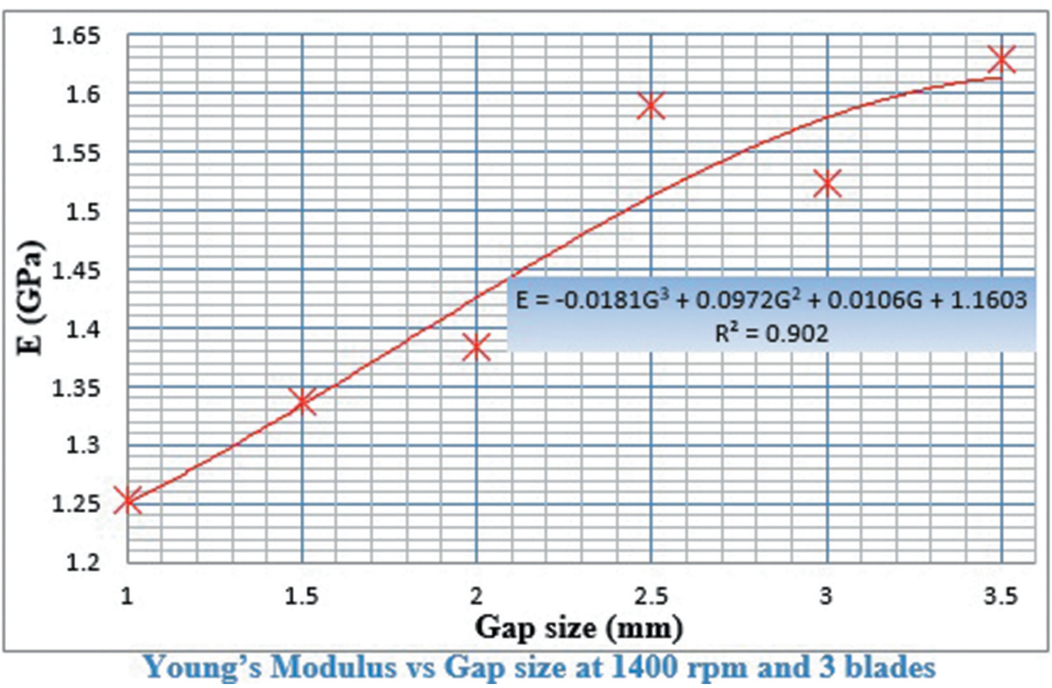

Figure 10. Variation of elastic modulus with gap size (extraction of fibers at 1400 rpm and 3 blades).

used single fibers that give higher strength compared to bundles (Kiruthika and Veluraja 2017; Senthilkumar et al. 2018). Moreover, the current study used the butt-end section that has the least properties (Chand 2008) hence lower than those reported by Kithiia, Munyasi, and Mutuli (2020) and Phologolo et al. (2012) for Kenyan fibers. The values are equally comparable to 200–400 MPa stress, 9–40 GPa modulus, and 2–14% strain reported by Haque et al. (2015) and 348 MPa stress, 3.8 GPa modulus, and 30% strain reported by Senthilkumar et al. (2018). Generally, the low values obtained are due to high lignin and hemicellulose content in Kenyan sisal fibers (Phologolo et al. 2012) that reduce the fiber strength.

Brushing improved the fiber grade to UG because the pins on brushing elements align the microfibrils with the fiber axis hence strengthening them (Petroudy 2017).[8] Brushing also removes curled and weak fibers and undecorticated pieces that reduce their overall strength. Furthermore, brushing reduces the effective diameter of the fibers hence better properties since a larger fiber diameter has an increased probability of finding a larger flaw that weakens the fiber (Inacio, Lopes, and Monteiro 2010).

When drum speed is increased from 900 to 1400 rpm at 12 blades and 2.5 mm gap size during extraction, the fracture stress drops by 40% (165 ± 8 to 99.6 ± 11 MPa, see Figure 3) and modulus by 46% (2.30 ± 0.12 to 1.24 ± 0.26 GPa, see Figure 4) while the fracture strain increases by 10% (0.073 ± 0.02 to 0.08 ± 0.02, see Figure 5). During brushing, the fracture stress drops by 21% (182 ± 0.002 to 144 ± 4 MPa, see Figure 6), modulus by 39% (2.46 ± 0.2 to 1.50 ± 0.02 GPa, see Figure 7) while the fracture strain increases by 30% (0.074 ± 0.002 to 0.096 ± 0.002, see Figure 8). When the speed increases, mechanical stresses on the fibers also increase thus weakening the bond between the matrix and microfibrils; a major cause of fiber failure (Bai et al. 2002). Furthermore, the increased stresses and the number of interactions between the blade and fibers damage the cuticle creating interfacial defects that acerbate fiber fracture (Petroudy 2017; Zhu, Hao, and Zhang 2018). Lastly, the excessive fiber grinding caused by the blades destroys the cell walls leading to low crystallinity; reduced crystallinity implies low strength and high elongation (Petroudy 2017). The correlation

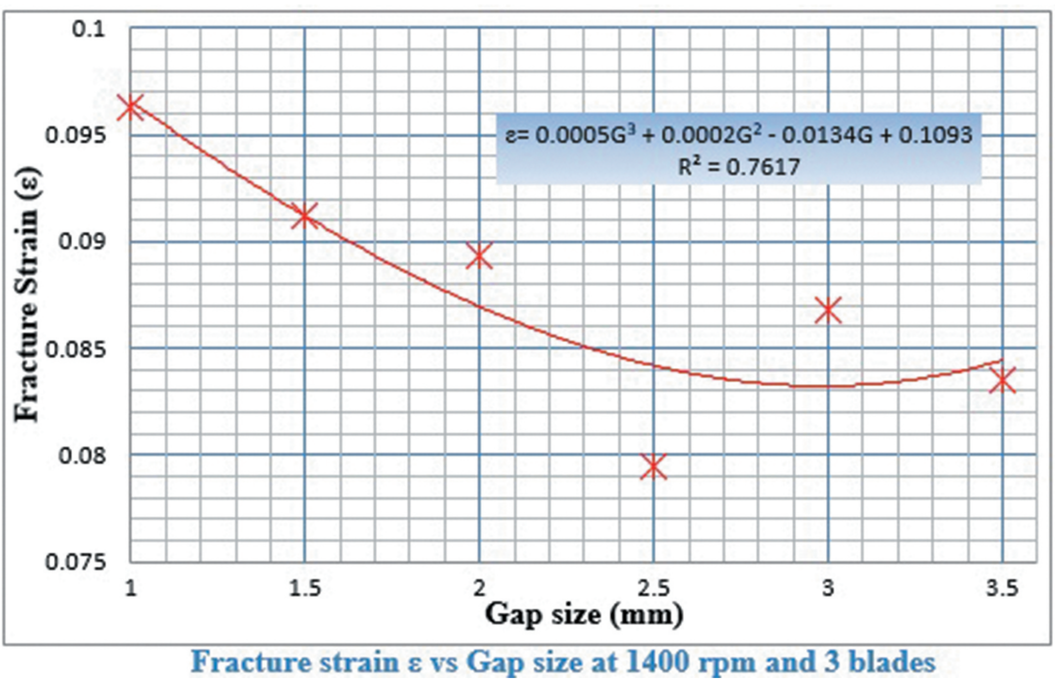

Figure 11. Variation of fracture strain with gap size (extraction of fibers at 1400 rpm and 3 blades).

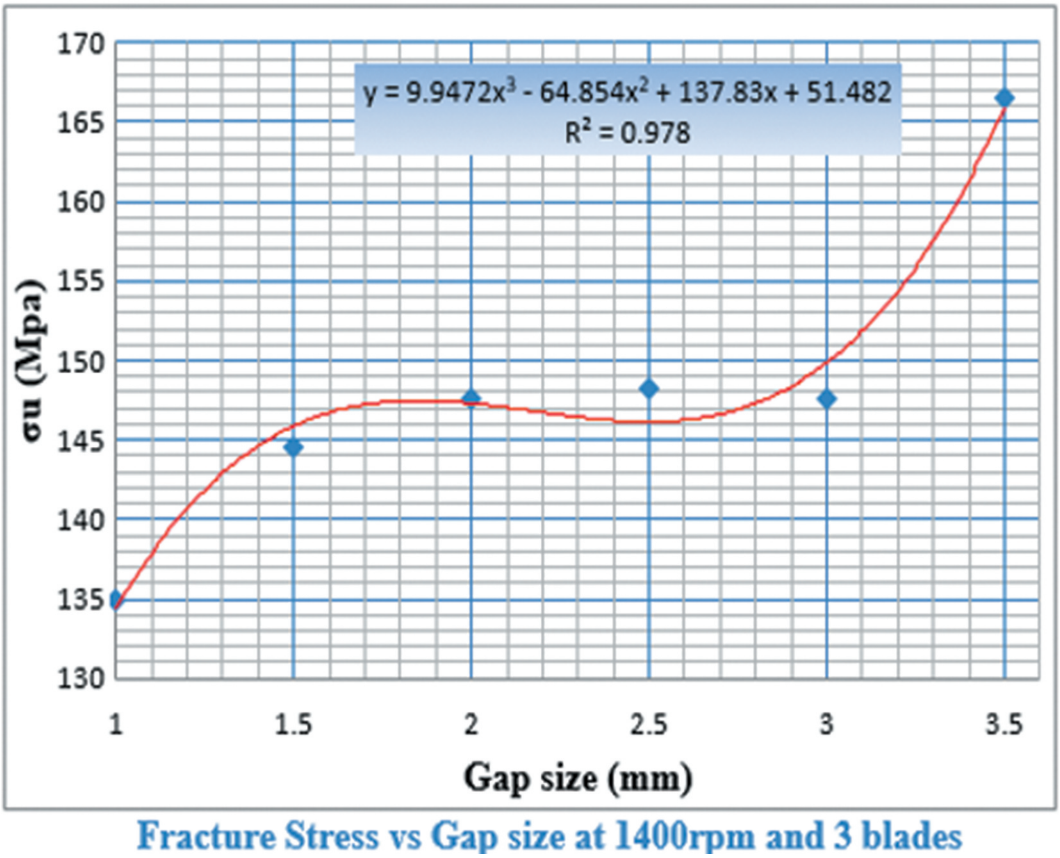

Figure 12. Variation of fracture stress with gap size (brushing of fibers at 1400 rpm and 3 brushing elements).

coefficients between stress, strain, and modulus and speed are 0.997, 0.974, and 1 (see Figure 3–5) respectively, for extraction and 0.980, 1, and 0.998 (Figure 6–8) respectively for brushing. This implies that the fibers are highly correlated with the processing drum speed.

During extraction, increasing the gap size from 1 to 3.5 mm at 3 blades and 1400 rpm increases stress by 7% (126.6 ± 11 to 135.1 ± 4 MPa, see Figure 9) and modulus by 30% (1.25 ± 0.16 to 1.63 ± 0.04 GPa, see Figure 10) but the fracture strain drops by 13% (0.096 ± 0.001 to 0.084 ± 0.01, see Figure 11). For brushing, the stress is increased by 23% (135 ± 18 to 166.6 ± 19 MPa, see Figure 12) and modulus by 18% (1.53 ± 0.16 to 2.38 ± 0.2 GPa, see Figure 13) whereas the fracture strain drops by 18% (0.088 ± 0.01 to 0.072 ± 0.01, see Figure 14). These results are so because when the gap size is increased, the clearance between the blades and the fiber is also increased thus reducing the severity of the blade stresses that would otherwise debond the matrix from the load-bearing microfibrils, damage the cuticle creating defects or grind the cell walls reducing fiber crystallinity. The correlation coefficients between stress, strain, and modulus and gap size are 0.990, 0.950, and 0.870 (see Figure 9–11) respectively for extraction and 0.990, 0.990, and 0.970 (see Figure 12–14) respectively for brushing. Hence, the extraction and brushing gap sizes have a significant influence on the properties of sisal fibers.

During extraction, increasing the number of extraction blades from 3 to 12 at 2.5 mm gap size and 1400 rpm reduces stress by 21% (126.6 ± 11 to 99.64 ± 11 MPa, see Figure 15) and modulus by 22% (1.59 ± 0.0.04 to 1.24 ± 0.3 GPa, see Figure 16) but increases fracture strain by 1.3% (0.079 ± 0.00 to 0.080 ± 0.02, see Figure 17). During brushing, increasing the number of brushing elements from 3 to 12 at 2.5 mm gap size and 1400 rpm reduces stress by 3% (148.2 ± 9 to 144.2 ± 4 MPa, see Figure 18)

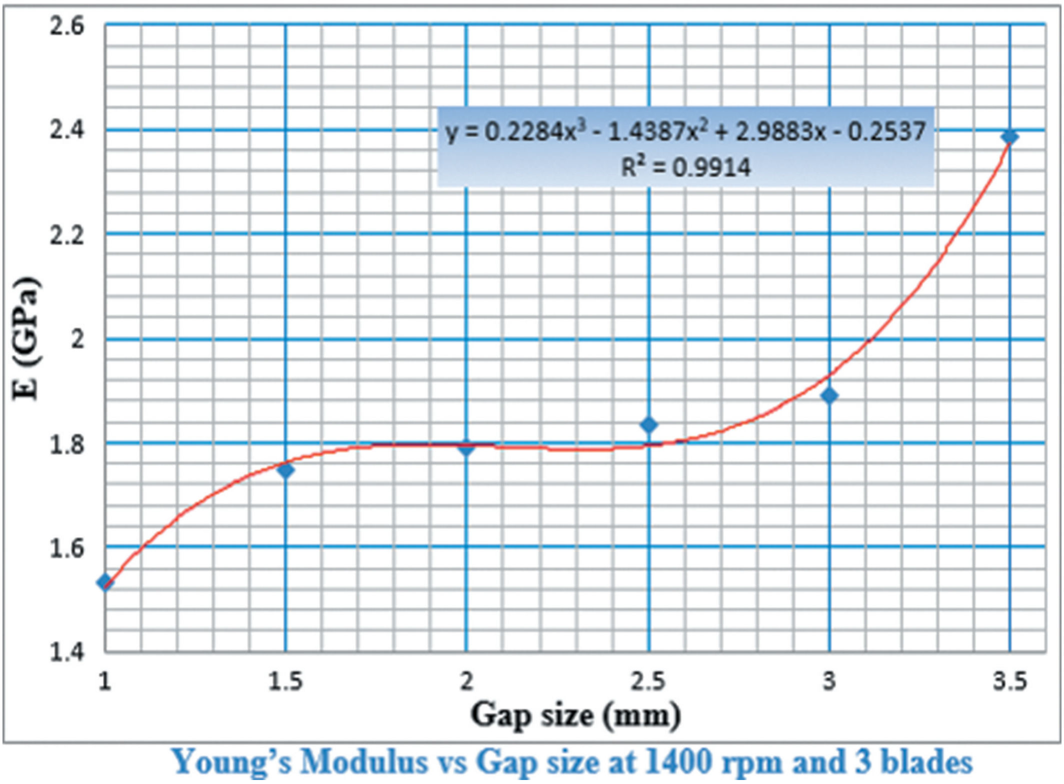

Figure 13. Variation of elastic modulus with gap size (brushing of fibers at 1400 rpm and 3 brushing elements).

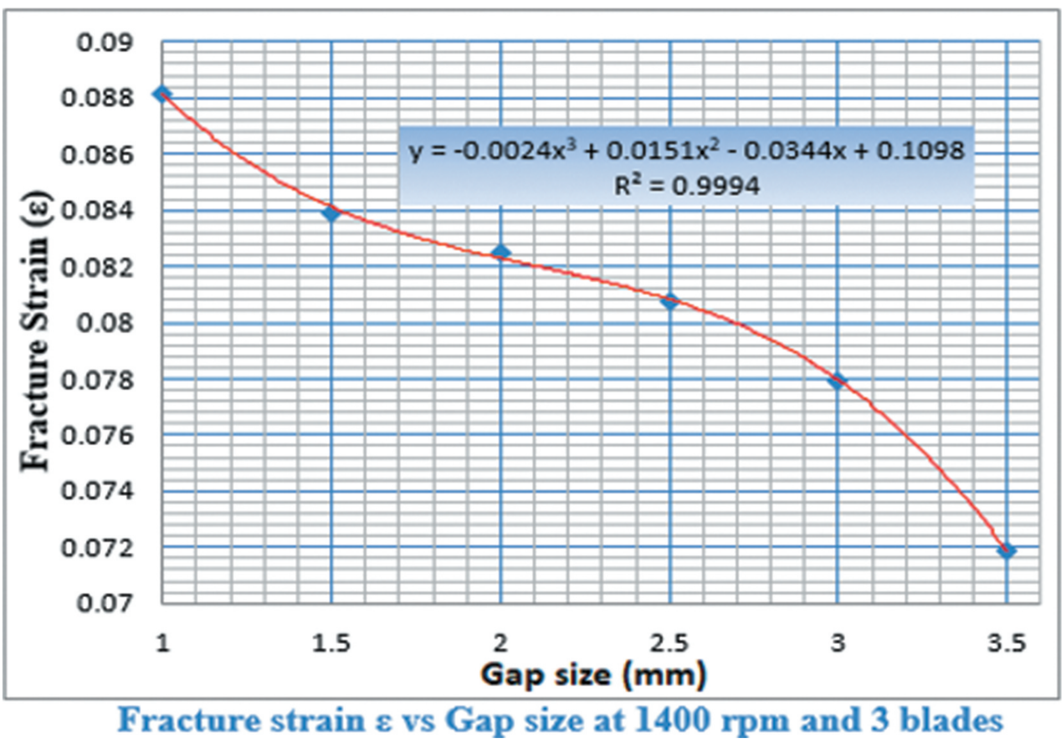

Figure 14. Variation of fracture strain with gap size (brushing of fibers at 1400 rpm and 3 brushing elements).

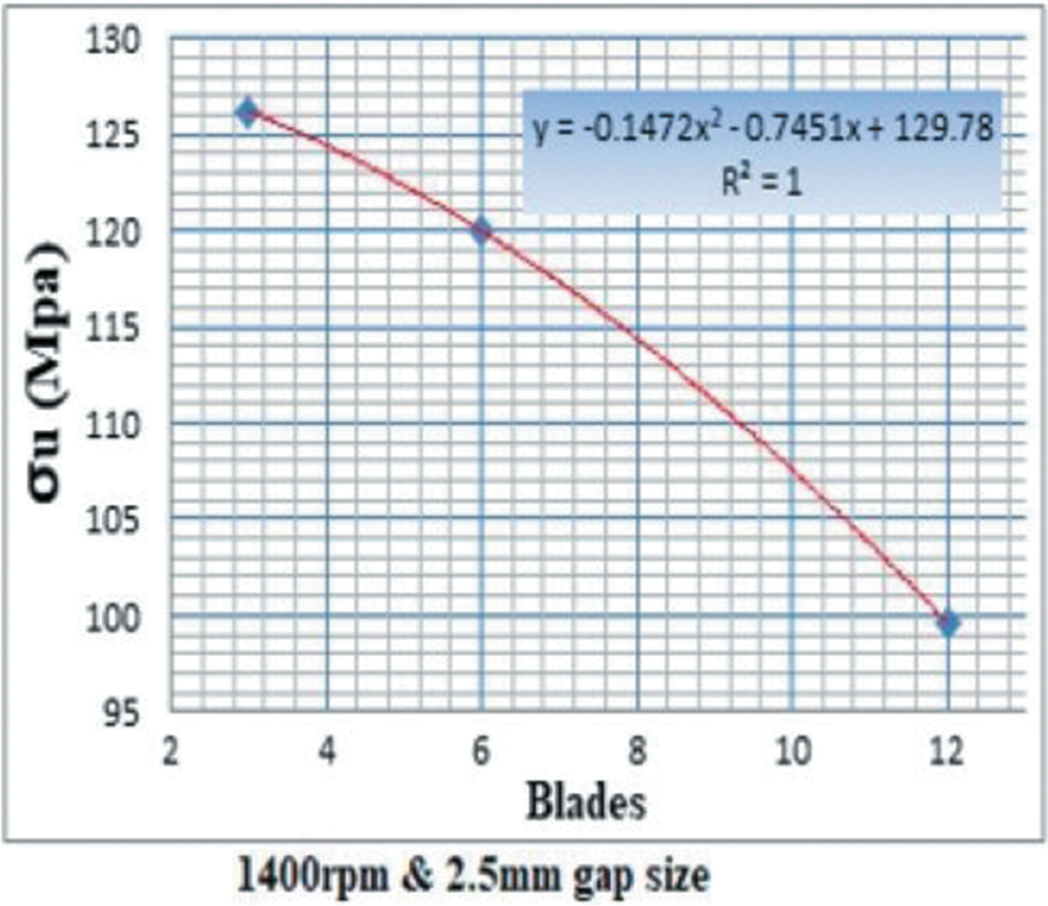

Figure 15. Variation of fracture stress with the number of blades (extraction of fibers at 1400 rpm and 2.5 mm gap size).

and modulus by 18% (1.83 ± 0.0.14 to 1.50 ± 0.02 GPa, see Figure 19) but increases fracture strain by 19% (0.081 ± 0.001 to 0.096 ± 0.002, see Figure 20). Increasing extraction blades and brushing elements also increase the blade stresses on fibers that are linked with debonding the matrix from the sub-fibers, damaging the cuticle, destroying the cell walls that reduce the degree of crystallinity and therefore strength. The correlation coefficients between stress, strain, and elastic modulus, and number of blades/brushing elements are all one for both processes (see Figure 15–20). Therefore, the properties greatly vary with the number of extraction blades and brushing elements.

In summary, the fiber properties are the poorest at lower gaps, higher speeds, and the higher number of blades/brushing elements. Brushed fibers have better tensile properties compared to unbrushed fibers. With these findings, it was argued that judicious decisions can be made by those endeavoring to design small-scale extraction/brushing machines or to use the sisal fibers for reinforcement purposes. The research has quantified the effects of the extraction and brushing parameters on the fracture stress, fracture strain, and elastic modulus of sisal fibers that are important properties used to determine the resultant properties of fiber-reinforced composites. Therefore, there is a need to pay attention to the appropriate processing method if the high properties of the sisal fibers are to be conserved.

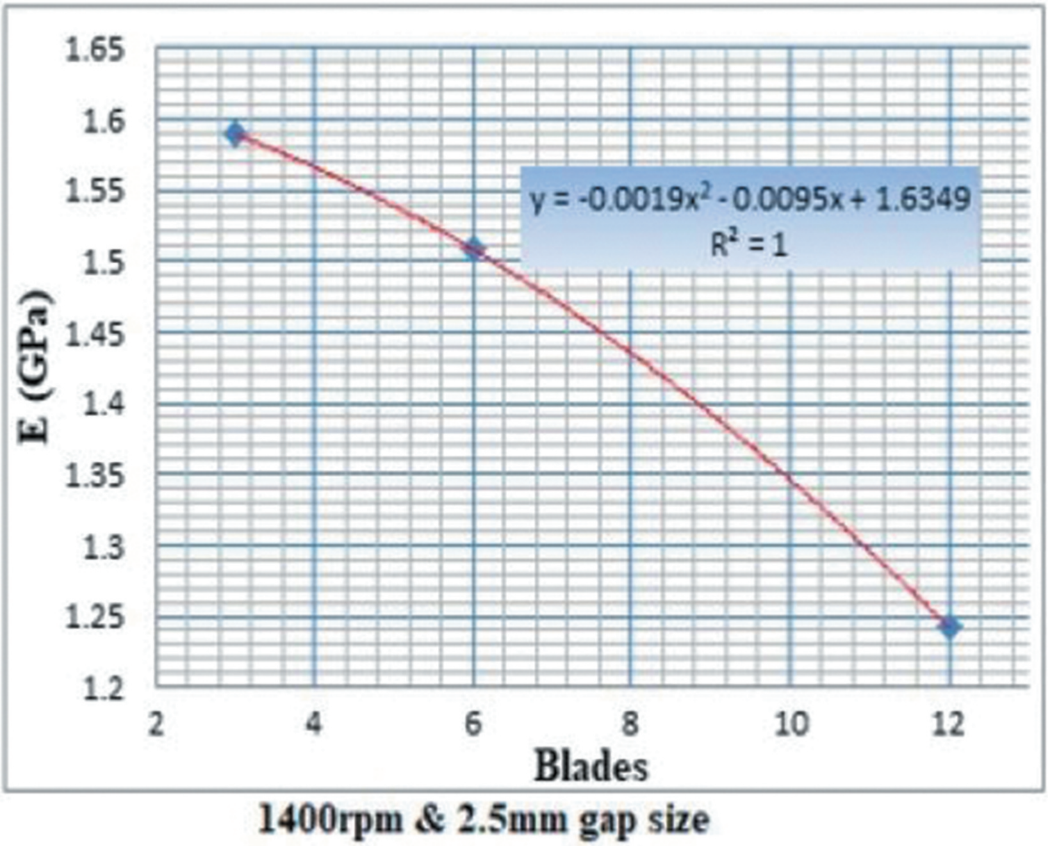

Figure 16. Variation of elastic modulus with the number of blades (extraction of fibers at 1400 rpm and 2.5 mm gap size).

Due to many samples used as a result of many processing variables under investigation, the study was limited to the butt-end section of the sisal leaf and a gauge length of 140 mm. Even though the properties of sisal fibers slightly vary with gauge length (Abir, Kashif, and Razzak 2015; Petroudy 2017), this did not affect the objective of the study of establishing the variation of fiber properties with processing variables because all other factors such as plant age, environmental conditions, gauge length, and temperature were kept constant.

Conclusion

The study concludes that;

- The processing variables have an influence on the properties of sisal fibers.
- The properties of sisal fibers highly correlate with the drum speed, gap size, and the number of extraction blades/brushing elements.
- The optimum properties are achieved at 6 blades, 1000–1200 rpm drum speed, and 1.5–2 mm gap size for the extraction process and at 3 brushing elements, 1000–1200 rpm drum speed and 2–3 mm gap size for brushing process.

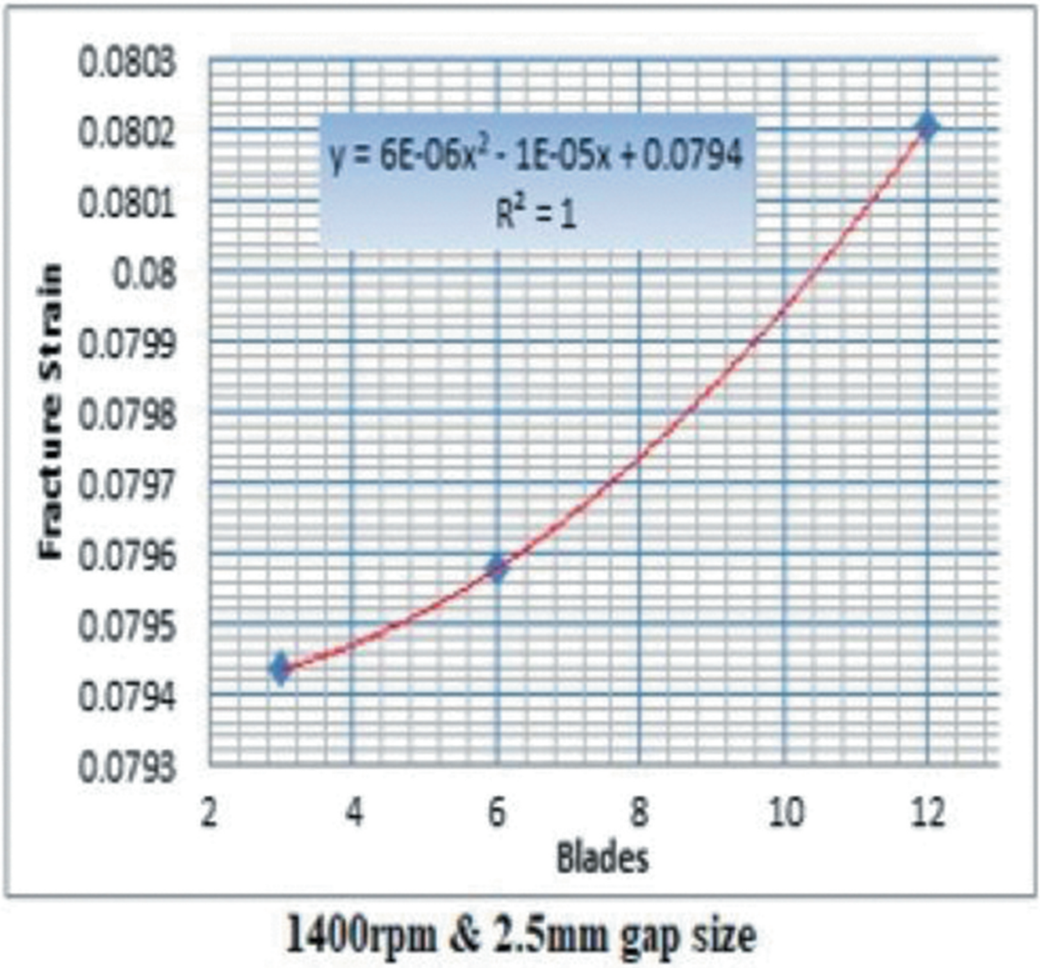

Figure 17. Variation of fracture strain with the number of blades (extraction of fibers at 1400 rpm and 2.5 mm gap size).

- Generally, the average mechanical properties of brushed fibers (σ = 142.68 ± 23 MPa, E = 1.776 ± 0.39 GPa and ε = 0.0812 ± 0.01) are better than those of unbrushed fibers (σ = 124.04 ± 19 MPa, E = 1.484 ± 0.28 GPa, and ε = 0.085 ± 0.012) for the same set of variables.
- Brushing of sisal fibers does not only improve the grade of sisal fibers but also the mechanical properties.

Acknowledgments

There are no acknowledgments at this point.

ORCID

N. W. Barasa http://orcid.org/0000-0003-4106-8629

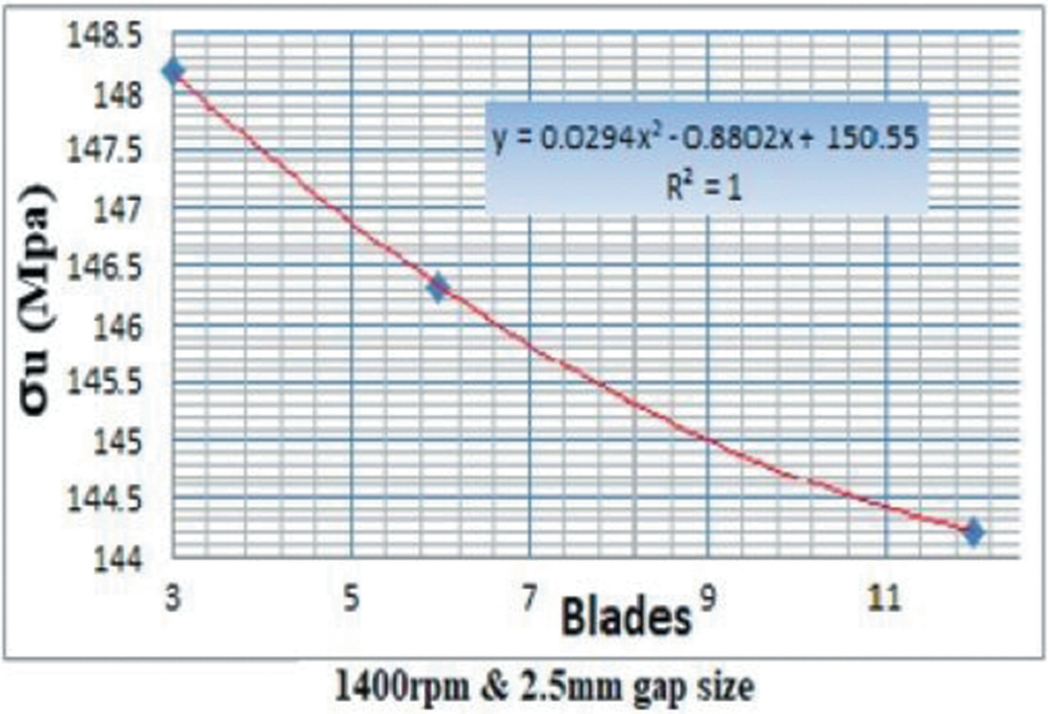

Figure 18. Variation of fracture stress with the number of brushing elements (brushing of fibers at 1400 rpm and 2.5 mm gap size).

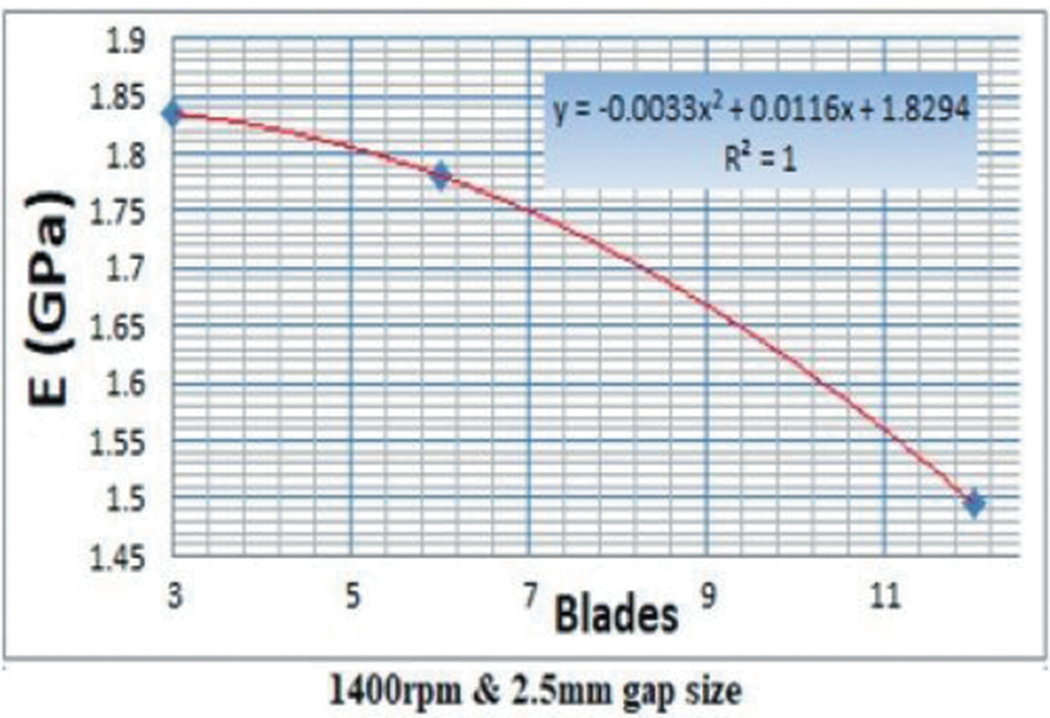

Figure 19. Variation of elastic modulus with the number brushing elements (brushing of fibers at 1400 rpm and 2.5 mm gap size).

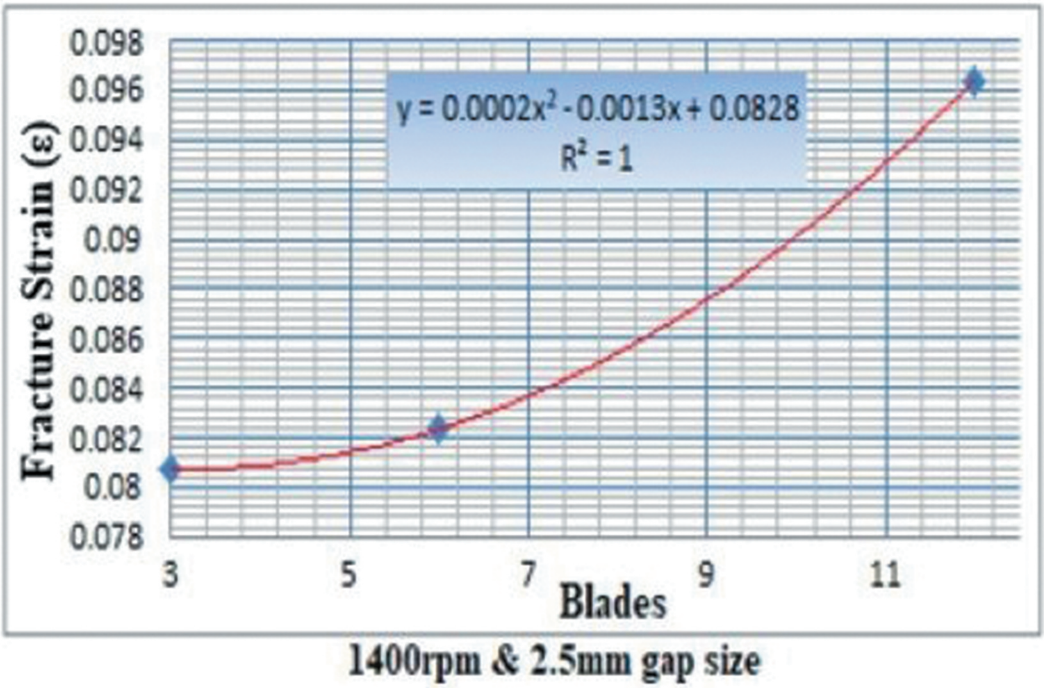

Figure 20. Variation of fracture strain with the number of brushing elements (brushing of fibers at 1400 rpm and 2.5 mm gap size).

Notes

1. Arid and Semi-Arid Lands.
2. The angle microfibrils make with the axis of the fiber.
3. A small-scale machine for scraping the fiber of henequen or sisal.
4. Sisal grown along the hedges of farms for demarcation.
5. Brushing element consisted of a steel blade with 25 steel comping pins, 2 mm diameter and evenly spot welded.
6. The ratio of average fiber length to the original leaf length.
7. Unwashed hand decorticated sisal.
8. Under grade.

Declaration of interest statement

The authors declare that there are no conflicts of interest that could have influenced the work reported in this paper.

Data availability statement

The primary data for the analysis and presentation of the findings in this study are available from the corresponding author upon reasonable request.

References

Abir, M. R., S. M. Kashif, and A. Razzak. 2015. Tensile and statistical analysis of sisal fibers for natural fiber composite manufacture. *Advanced Materials Research* 1115:349–52. doi:10.4028/www.scientific.net/AMR.1115.349.

ASTM (American Society for Testing and Materials). 2008. *C1557: Standard test method for tensile strength and Young's modulus of fibers*. West Conshohocken, USA: American Society for Testing and Materials.

Bai, S. L., R. K. Y. Li, Y. W. Mai, and C. M. L. Wu. 2002. Morphological study of sisal fibers. *Advanced Composites Letters* 11 (3):133–40. doi:10.1177/096369350201100304.

Bhowmicka, M., S. Mukhopadhyayb, and R. Alagirusamyb. 2012. Mechanical properties of natural fiber-reinforced composites. *Textile Progress* 44 (2):85–140. doi:10.1080/00405167.2012.676800.

Chand. 2008. Sisal reinforced polymer composites. In *Tribology of natural fiber polymer composites*, 84–107. Sawston, Cambridge: Elsevier. doi:10.1533/9781845695057.84.

Denscombe, M. 2010. *The good research guide: For small-scale social research projects*. 4th ed. Berkshire: McGraw-Hill Education.

Ferreira, D. C. O., A. S. Ferreira, and S. N. Monteiro. 2018. Weibull analysis of tensile tested piassava fibers with different diameters. *Revista Matéria* 23 (4):1–11. doi:10.1590/s1517-707620180004.0588.

Fidelis, M. E., T. V. Pereira, O. Gomes, F. A. Silva, and R. D. Filho. 2013. The effect of fiber morphology on the tensile strength of natural fibers. *Journal of Materials Research and Technology* 2 (2):149–57. doi:10.1016/j.jmrt.2013.02.003.

Gobikannan, T., H. Berihun, E. Aklilu, S. J. Pawar, G. Akele, T. Agazie, and S. Bihonegn. 2020. Development and characterization of sisal fiber and wood dust-reinforced polymeric composites. *Journal of Natural Fibers*:1–10. Advance online publication. doi:10.1080/15440478.2019.1710649.

Haque, R., M. Saxena, S. C. Shit, and P. Asokan. 2015. Fibre-matrix adhesion and properties evaluation of sisal polymer composite. *Fibers and Polymers* 16 (1):146–52. doi:10.1007/s12221-015-0146-2.

Inacio, W. P., F. P. D. Lopes, and S. N. Monteiro. 2010. Diameter dependence of tensile strength by Weibull analysis: Part III sisal fiber. *Matéria (Rio De Janeiro)* 15 (2):124–30. doi:10.1590/S1517-70762010000200006.

Jain, N., M. Banerjee, and S. Sanyal. 2012. Effect of fiber length variations on properties of coir fiber reinforced cement-albumen composite (CFRCC). *IIUM Engineering Journal* 12 (1):63–76. doi: 10.31436/iiumej.v12i1.116.

Kayumba, V. A., M. Bratveit, Y. Mashalla, and B. E. Moen. 2007. Acute respiratory symptoms among sisal workers in Tanzania. *Occupational Medicine* 57 (4):290–93. doi:10.1093/occmed/kqm004.

Kiruthika, A. V., and K. Veluraja. 2017. Physical properties of plant fibers (sisal, coir) and its composite material with tamarind seed gum as low-cost housing material. *Journal of Natural Fibers* 14 (6):801–13. doi:10.1080/15440478.2017.1279104.

Kithiia, M. W., M. D. Munyasi, and M. S. Mutuli. 2020. Strength properties of surface modified Kenyan sisal fibers. *Journal of Natural Fibers*:1–11. Advance online publication. doi:10.1080/15440478.2020.1807446.

LSA (London Sisal Association). 2016. East African sisal fiber definitions. Accessed June 03, 2019. https://www.londonsisalassociation.org/kenya.php#

Majesh, M., and J. Pitchaimani. 2016. Dynamic mechanical analysis and free vibration behavior of intra-ply woven natural fiber hybrid polymer composite. *Journal of Reinforced Plastics and Composites* 35 (2):28–42. doi:10.1177/0731684415611973.

Mohammed, F., and N. Chan. 2008. Sisal reinforced polymer composites. In *Tribology of natural fiber polymer composites*, 84–107. Sawston, Cambridge: Elsevier. doi:10.1533/9781845695057.84.

Mokaloba, N., and R. Batane. 2014. The effects of mercerization and acetylation treatments on the properties of sisal fiber and its interfacial adhesion characteristics on polypropylene. *International Journal of Engineering, Science and Technology* 6 (4):83–97. doi:10.4314/ijest.v6i4.9.

Mutuli, S. M., T. J., Bessell, and E. S. J., Talitwala. 1982. The potential of sisal as a reinforcing fiber in cement base materials. African<italic> Journal of Science and Technology (ANST)</italic>, 1(1), 5–16.

Naik, R. K., R. C. Dash, and A. K. Goel. 2013. Mechanical properties of sisal (A. Sisalana) relevant to harvesting and fiber extraction. *International Journal of Agricultural Engineering* 6 (2):423–26.

Petroudy, D. S. R. 2017. Physical and mechanical properties of natural fibers. In *Mizi Fan and Feng FuAdvanced high strength natural fibre composites in construction*, 59–83. Iran: Elsevier. doi:10.1016/B978-0-08-100411-1.00003-0.

Phologolo, T., C. Yu, J. I. Mwasiagi, N. Muya, and Z. F. Li. 2012. Production and characterization of Kenyan sisal. *Asian Journal of Textile* 2 (2):17–25. doi:10.3923/ajtl.2012.17.25.

Rajkumar, D. R., K. Santhy, and K. P. Padmanaban. 2020. Influence of mechanical properties on modal analysis of natural fiber reinforced laminated composite trapezoidal plates. *Journal of Natural Fibers*:1–17. Advance online publication. doi:10.1080/15440478.2020.1724230.

Senthilkumar, K., I. Siva, N. Rajini, J. T. W. Jappes, and S. Siengchin. 2018. Mechanical characteristics of tri-layer eco-friendly polymer composites for interior parts of aerospace application. In *Sustainable composites for aerospace applications*, 35–53. Sawston, Cambridge: Elsevier. doi:10.1016/B978-0-08-102131-6.00003-7.

Silva, F. A., N. Chawla, and R. D. Filho. 2008. Tensile behavior of high performance natural (sisal) fibers. *Composites Science and Technology* 68 (15–16):3438–43. doi:10.1016/j.compscitech.2008.10.001.

Susheel, K., B. S. Kaith, and K. Inderjeet. 2009. Pretreatments of natural fibers and their application as reinforcing material in polymer composites: A review. *Polymer Engineering and Science* 49 (12):53–72. doi:10.1002/pen.21328.

Zhu, Z., M. Hao, and N. Zhang. 2018. Influence of contents of chemical compositions on the mechanical property of sisal fibers and sisal fibers reinforced PLA composites. *Journal of Natural Fibers* 17 (1):101–12. doi:10.1080/15440478.2018.1469452.

Appendix A

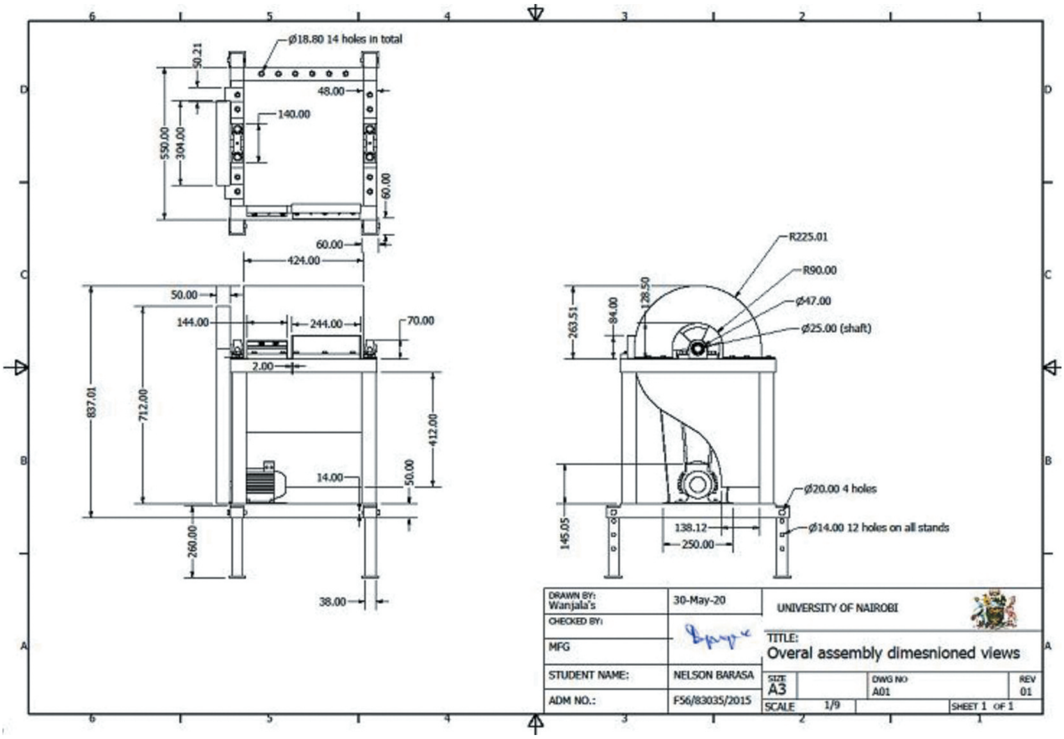

Figure A1. Views and dimensions of the raspador

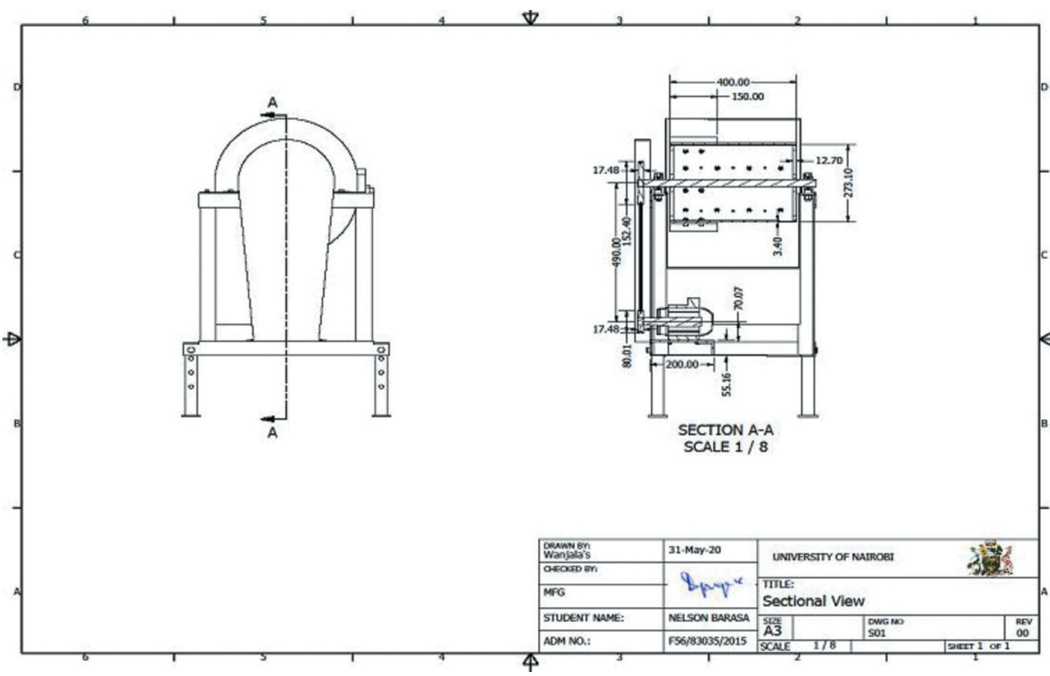

Figure A2. Sectional view (Section AA).